

Agentic Structured Graph Traversal for Root Cause Analysis of Code-related Incidents in Cloud Applications

Shengkun Cui[†], Rahul Krishna[‡], Saurabh Jha[‡], and Ravishankar K. Iyer[†]

[†]University of Illinois at Urbana-Champaign, Urbana, IL 61801, USA

[‡]IBM Research, Yorktown Heights, NY 10598, USA

Abstract—Cloud incidents pose major operational challenges in production, with unresolved production cloud incidents cost on average over \$2M per hour. Prior research identifies code- and configuration-related issues as the predominant category of root causes in cloud incidents. This paper introduces PRAXIS, an orchestrator that manages and deploys an agentic workflow for diagnosing code- and configuration-caused cloud incidents. PRAXIS employs an LLM-driven structured traversal over two types of graph: (1) a service dependency graph (SDG) that captures microservice-level dependencies; and (2) a hammock-block program dependence graph (PDG) that captures code-level dependencies for each microservice. Compared to state-of-the-art ReAct baselines, PRAXIS improves RCA accuracy by up to $3.1\times$ while reducing token consumption by $3.8\times$. PRAXIS is demonstrated on a set of 30 comprehensive real-world incidents that is being compiled into an RCA benchmark.

Index Terms—Cloud computing, agentic approach, incident diagnosis, root-cause analysis, program analysis, reliability

I. INTRODUCTION

Production cloud incidents cost on average over \$2M per hour [1], [2]. While operational mitigation actions such as reboot, restart, scale-out, and rollback can resolve many such incidents, approximately 24% remained unresolved by operational mitigation [3]. In those cases, engineers supported by tools must perform *root-cause analysis* (RCA)—a diagnostic process that identifies the origin (i.e., root causes) of the failure. When RCA is ineffective, outages can be prolonged and highly disruptive [4]–[7].

This paper introduces **PRAXIS**, an orchestrator that manages and deploys an agentic workflow for diagnosing code- and configuration-caused cloud incidents. PRAXIS employs a large language model (LLM)-driven structured traversal over two types of graph: (1) a service dependency graph (SDG) that captures microservice-level dependencies; and (2) a hammock-block [8], [9] program dependence graph (PDG) that captures code-level dependencies for each microservice. Together, these graphs efficiently encode microservice- and code-level dependencies. By explicitly and jointly imposing both microservices and code dependency structures in the agentic RCA workflow, PRAXIS extends the diagnosis beyond observability symptoms, making it capable of identifying and explaining root causes that lie in code or configurations. We demonstrate the breadth of PRAXIS using 30 real-world examples, integrated into a comprehensive benchmark which is in the process of being open-sourced.

Contribution. Our main contributions are as follows:

- 1) **PRAXIS**, an agentic approach for cloud incident RCA with structured, LLM-driven graph reasoning and traversal by utilizing microservices and program dependency graphs.
- 2) An application of the hammock block program dependence graph for agentic RCA, leveraging the hammock block’s hierarchical nesting structure to analyze microservice code at multi-granular levels seamlessly.
- 3) Code-Cloud-RCA Benchmark consisting of 30 different scenarios and each incorporating a unique software, configuration, deployment, or resource-related fault observed in the real-world [3]–[5], [10]–[13], and injected in a live Kubernetes cloud environment.
- 4) A demonstration of PRAXIS’s agentic capabilities to perform cross SDG-PDG traversal to diagnose a challenging incident.

Results. We evaluated the PRAXIS’s RCA effectiveness in terms of root cause accuracy and token consumptions across those 30 scenarios. PRAXIS achieved a root-cause reasoning accuracy of 61.5% and a root-cause identification accuracy of 73.9%, an increase of $3.1\times$ and $2.1\times$, respectively, over state-of-the-art ReAct baselines [14]–[16] using the most recent LLMs. In addition, PRAXIS reduced token consumption by $3.8\times$ from 624.4k tokens to 166.5k tokens per successful diagnosis, when comparing to the same baselines.

An important reason for PRAXIS’s effectiveness gain is its ability to reduce the context space and focus microservice- and code-level analysis on the regions most implicated by an incident, guided by the underlying dependency structure. Prior work [14]–[19] does not impose such a structure and relies entirely on the LLM’s built-in autoregressive analysis over unstructured, plain-text prompts, which is shown to be less effective. PRAXIS instead explicitly constrains the LLM’s reasoning along graph-defined dependencies encoded by PDG and SDG via LLM-driven graph traversal.

PRAXIS stands at the intersection of cloud incident diagnosis (an SRE task) and program analysis (an SWE task)¹. By jointly investigating microservice-level and code-level dependencies—a process we refer to as *Cross-SDG-PDG traversal*—PRAXIS can diagnose incidents whose fault chains interleave microservice and code dependencies across multiple hops. This unique capability distinguishes PRAXIS from existing approaches, which typically limit their investigation to either the microservice level using observability data [14]–[18], [20] or the code level

¹SRE: site reliability engineering; SWE: software engineering.

based on engineer-curated postmortem issue tickets [19]. We demonstrate this capability of PRAXIS in §III.

II. TERMINOLOGY

Root cause analysis (RCA). Following the understanding espoused in [21], RCA is the diagnostic process that (a) identifies the microservice responsible for the incident, and (b) the statement(s), function(s), or configuration(s) identifying the origin of the incident, and (c) provide a concise reasoning of its manifestation to facilitate remediation.

Service dependency graph (SDG) Service dependency graph of a cloud application is a directed graph with nodes representing individual microservices or associated resources (e.g., pods, configMaps) and directed edges showing the dependency between them. In any given interval, the graph represents the current dynamics among the microservices.

Program dependence graph (PDG). A directed graph that captures microservice program structure [22], the nodes are hammock blocks [8], [9] and the edges are data, control, and call dependencies.

Hammock block. A hammock block is used to restructure unstructured code into a structured block format into a single-entry-single-exit (SESE) region [8], [9].

Observability. Observability with respect to microservices is the ability to understand the internal state of a distributed system by examining its generated data (e.g., logs, metrics, events, and distributed traces) via data analysis to gain real-time insights.

Code context. Code context refers to code-related information.

III. APPROACH OVERVIEW

This section introduces PRAXIS, an orchestrator that manages and deploys an agentic workflow for cloud incident RCA. At the core this approach is an LLM-driven structure traversal over two types of graph: (1) a SDG that captures microservice-level dependencies—providing a high-level localization of faulty microservices; and (2) a hammock-block PDG that captures code-level dependencies for each microservice—allowing for fine-grained RCA decisions that identify offending code paths and configurations responsible for the incident. PRAXIS’s hammock-block PDG provides an efficient structural representation of a microservice program, enabling seamless analysis of microservice code at different granularities. By integrating tools, observability data, and dependency graphs, PRAXIS delivers demonstratively accurate RCA for live cloud incidents, demonstrated on microservice-based Kubernetes applications. In summary the core functionalities of PRAXIS’s workflow include:

Data gathering. Like prior agentic approaches [14]–[20], PRAXIS uses cloud monitoring tools [23]–[25] to actively collect a set of automated and user-specified alerts referred to as *golden-signal alerts* (e.g., error-rates or latencies exceeding user-defined thresholds) and observability data consisting of cloud application and microservice logs, distributed traces of microservice calls, Kubernetes events, and application metrics.

PRAXIS also actively retrieves microservice topology, as in [26], [27], using a cloud topology monitoring platform [28], which is used to build the SDG. In addition, PRAXIS uses microservice codebases for constructing PDG for microservices.

SDG and PDG construction. As the key differentiator from prior work [15], [19], PRAXIS’s agentic workflow utilizes two modalities of graphs. The first is a dynamically evolving service dependency graph [26], [27] for the cloud application, with currently deployed microservices as nodes and inter-microservices dependencies as edges, generated via a real-time topology monitor [28]. The second is a hammock-granularity PDG for each microservice node in the SDG, with hammock blocks as nodes and control, data, and function-call dependencies as edges. This PDG is generated by static program analysis tools [29], [30] and represents the software dependency of a microservice application relevant to root-cause analysis.

Together, the SDG and PDG capture relevant microservice-level and code-level dependencies for RCA. These graphs serve as bases for RCA via LLM-driven graph traversal, first at the microservice level and subsequently at the code level, to identify responsible microservices, faulty code sites, and/or configurations that might explain the observed erroneous signals (such as active alerts, error logs, traces, metrics, and events), providing in-depth RCA down to the code level.

Structure-aware agentic RCA. Upon triggering by active golden-signal alert(s), PRAXIS presents the relevant data (active alert(s) and error traces) to an LLM to identify and select microservices correlated with error signals in those data. The selected microservices become initial candidates for agentic focus. Subsequently, the LLM investigates each microservice by performing structure-aware reasoning through traversal of the corresponding hammock blocks. PRAXIS uniquely constructs the PDG using hammock blocks at different granularities spanning module, class, function, and statement levels, allowing the LLM to seamlessly move between levels as required to optimize analysis efficiency and accuracy. Leveraging this structure, the LLM iteratively traverses first the SDG and then the hammock-block PDG at the required level to narrow down the pool of potentially responsible microservices and the corresponding fault sites in code or configuration, until it reaches a conclusive decision on the root cause.

Unlike prior agentic approaches that process code as monolithic text [15], [19] for RCA, PRAXIS provides an efficient approach for strategically traversing the SDG and the corresponding hammock blocks in PDG, analyzing local code context alongside observability data. The graph traversal constrains the LLM’s diagnosis to incident-relevant dependency paths and accumulates code insights that could explain the observed error signals (e.g., alerts, error traces, error logs), while filtering out irrelevant paths. Thus, instead of relying solely on the LLM’s attention mechanism to implicitly infer code structure and focus on context relevant to the incident, PRAXIS’s workflow explicitly imposes structure-aware, concise, and accurate diagnosis of the underlying incident. Based on the observability data and the accumulated code insights, the LLM

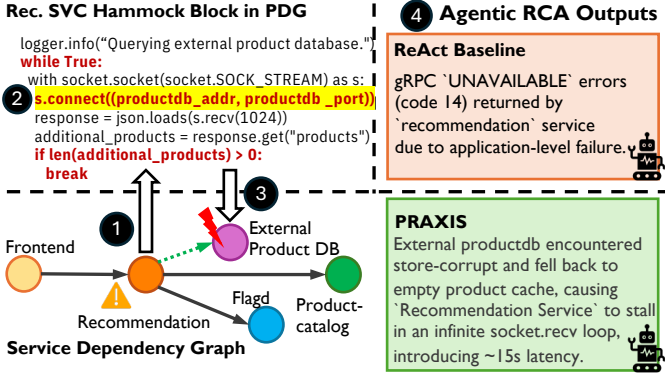


Fig. 1: **Incident:** Degraded external database returned empty responses, triggering a silent retry loop in the Recommendation service that manifested solely as high latency alert associated with the Recommendation service, without explicit error logs or error traces. **Cross-SDG-PDG traversal:** (1) LLM selects the Recommendation service for investigation based on the observed alert. (2) Investigation of the Recommendation service reveals a silent retry loop with missing error logs. Code traversal shows that an unresponsive External Product Database triggers this loop. (3) Subsequent investigation shows a storage failure in the External Product DB as the root cause. (4) The ReAct agent baseline fails to pinpoint the precise root cause, whereas PRAXIS successfully isolates the root cause.

classifies the microservice under investigation as PRIMARY FAILURE, SYMPTOM ONLY, or UNRELATED. Upon finishing its investigation of the current microservice, PRAXIS moves on to investigate the other selected microservices and the dependees according to the SDG. Once all initially selected microservices and their dependees have been investigated, PRAXIS calls the LLM to consolidate the per-microservice investigation decision into a final RCA report detailing the fault's origin, propagation, and impact.

Cross-SDG-PDG traversal: a challenging scenario. A key innovation of our approach is the ability to handle incidents where multiple microservices are identified as potential root causes. In such cases, the LLM must traverse from the first microservice into its specific hammock block within the PDG, and then transition to a second microservice according to the SDG and its respective hammock blocks to form a coherent and holistic RCA decision. PRAXIS facilitates this by attaching the PDG of each microservice to the global SDG, ensuring the LLM can perform these cross-layer traversals when needed. We demonstrate the necessity of this unique capability in Figure 1, using a challenging incident that the baseline ReAct agent failed to solve.

As shown by the agent output (Figure 1-4), the ReAct baseline (equipped with SRE and SWE tools) concludes its diagnosis at the Recommendation service after inspecting its code (Figure 1-2). In contrast, PRAXIS executes a cross-SDG-PDG traversal: it pivots its investigation from code-level (PDG) back to the microservice-level (SDG) to identify the external database dependency (Figure 1-3), where it repeats the investigation process to identify the failed database as

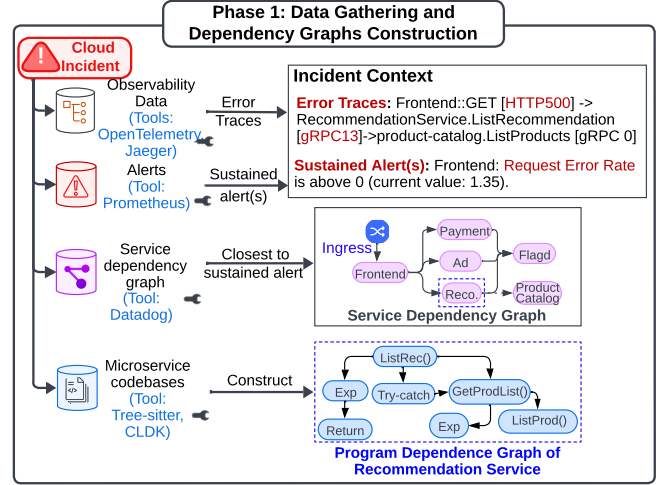


Fig. 2: PRAXIS Phase 1: Data gathering and dependency graph construction.

the root cause, aligning with the groundtruth. This example demonstrates that merely equipping a ReAct SRE agent with SWE/code tools, or treating the two domains independently (e.g., by straightforwardly composing SRE and SWE agents), yields suboptimal results. Those approaches fail because they lack a structure in decision-making to explicitly enforce the investigation of the next dependencies, causing them to prematurely conclude the investigation before arriving at the actual root cause—a critical gap that PRAXIS addresses.

IV. PRAXIS: METHODOLOGY

This section details the methodology of PRAXIS, which employs an iterative reasoning process to perform RCA on cloud incidents. PRAXIS operates in the following phases:

Phase 1 (§IV-A, Figure 2): Data gathering and dependence graph construction. PRAXIS collects the *incident context*: error traces from Jaeger [24], sustained alerts from Prometheus [23], the SDG snapshot from the cloud topology monitoring platform [28], and PDG from the microservice source code using Tree-sitter [29] and CLDK [30].

Phase 2 (§IV-B, Figure 3): Microservice Candidate(s) Selection. Using the incident context (i.e., error traces and sustained alerts), PRAXIS employs an LLM to identify initial *root-cause candidate* microservices.

Phase 3 (§IV-C, Figures 4 and 5): RCA decision-making. PRAXIS directs an LLM to iteratively traverse the microservice's PDG to construct *program context* and diagnose code regions relevant to the incident, then assign an RCA judgment (PRIMARY FAILURE, SYMPTOM ONLY, or UNRELATED) before advancing to the next microservice as suggested by the SDG.

Phase 4 (§IV-D, Figure 6): Final RCA summary. Upon completing all investigations, PRAXIS consolidates the LLM's judgments and reasoning to generate a comprehensive RCA report (Figure 6) that provides (1) root-cause identification and (2) root-cause reasoning down to the responsible statements, functions, or configurations.

A. Phase 1: Data Gathering

In Phase 1 (Figure 2) of the agentic RCA workflow, PRAXIS leverages cloud monitoring tools [23]–[25] to actively monitor alerts (e.g., error rates, latency). Upon detecting a sustained alert indicating a sustained SLO violation, it collects and aggregates the relevant observability data to construct the *incident context*, as detailed below.

- 1) *Alerts*. Alerts signal service-level objective (SLO) violations, including high latencies and elevated error rates. PRAXIS continuously polls the Prometheus API for any active sustained alerts; these alerts serve as the initial triggers for PRAXIS’s RCA workflow.
- 2) *Distributed error traces*. Distributed error traces record runtime request latencies and propagations of inter-service requests, explicitly highlighting error dependency paths across microservice boundaries.
- 3) *Logs*. Cloud application and microservices log entries and their associated error/warning patterns². These logs provide rich runtime context (e.g., information, warnings, errors, stack traces, exceptions), offering direct insight into the timing and nature of runtime executions, errors, and failures.
- 4) *Events*. Kubernetes events regarding deployment updates and lifecycle changes that affect the microservice or its resources (e.g., ReplicaSet scaling, container restarts), providing diagnostic context on deployment/resource configuration changes that could reveal the root cause.
- 5) *Metrics*. Aggregated error and warning counts derived from logs and events, alongside span and trace latency measurements to quantify the severity of observed anomalies.

PRAXIS aggregates sustained alerts and error traces into the incident context, which serves as the initial description of the cloud incident. While pre-collected, logs, metrics, and events will be used in Phase 3 for per-microservice investigation.

Figure 2 illustrates an example incident context for a cloud incident in which the Frontend service is unable to recommend products: (1) a sustained Request Error Rate alert is observed in the Frontend service, and (2) the corresponding error traces reveal gRPC13 errors during calls to the Recommendation.ListRecommendation endpoint.

SDG & PDG PRAXIS’s agentic workflow utilizes two graphs: (1) a dynamically evolving SDG for the cloud application, representing the current microservices configuration that is being deployed and executed; and (2) a hammock-block PDG for each microservice node in the SDG, representing the software dependency of a microservice program relevant to root-cause analysis. Together, these graphs capture relevant microservice-level and code-level dependencies and serve as bases for agentic RCA via LLM-driven graph traversal. PRAXIS constructs these graphs in Phase 1 after gathering data, as shown in Figure 2.

a) *Service Dependency Graph (SDG)*: PRAXIS employs a *service dependency graph* (SDG) to capture the currently

deployed microservices and their dependencies at the time of the incident. A *SDG* models the dependency structure of a cloud application $C = \{e_1, \dots, e_n\}$, where each e_i is a microservice or one of its associated resources (pod or ConfigMap) [26], [27]. It is defined as a directed graph $G_C = (V, E_{\text{depend}}, \lambda_V)$ with $V = C$, where an edge (u, v) indicates that microservice u depends on v (another microservice or one of its resources), and non-microservice nodes serve as leaves with no outgoing edges. Each node is annotated by λ_V to record its kind and name, completing the definition of the SDG. The SDG G_C is constructed and maintained by a cloud topology monitor [28]. To capture the dynamic nature of the cloud environment, the graph is updated at predefined intervals. Consequently, PRAXIS retrieves the graph snapshot at the time of the alert to bootstrap the RCA process. Since the investigation can extend to non-microservice cloud components such as a pod or a configMap associated with a microservice, we hereinafter refer to a node in the SDG as an *entity*. Figure 2 presents an example SDG³ of the cloud application [31] employed by our benchmark.

b) *Program dependence graph (PDG)*: To perform fine-grained diagnosis, PRAXIS augments each microservice node in the SDG with a *program dependence graph* (PDG) [22], enabling reasoning over code paths and potential fault sites. For a microservice program P comprising a finite set of single-entry–single-exit (SESE) hammock blocks $B = \{b_1, \dots, b_n\}$ [8], [9], the PDG is defined as a labeled directed graph $G_P = (V, E, \lambda_V, \lambda_E, \prec)$. Here, $V = B$, and edges $E = E_{\text{ctl}} \cup E_{\text{data}} \cup E_{\text{call}}$ capture control-, data-, and call-dependence between blocks; λ_V and λ_E annotate nodes and edges with their corresponding semantic attributes. A containment relation \prec specifies when one hammock block syntactically contains another, inducing a hierarchical structure spanning module-, class-, function-, and statement-level regions. This hierarchy allows PRAXIS to traverse and reason about the program at whatever granularity is most informative for RCA.

Provided with the microservice codebases, PRAXIS automatically generates the PDG for microservices as part of the initialization process, using static program analysis tools: Tree-sitter [29] for parsing hammock blocks and CLDK [30] for data, call, and control relationship analysis. The PDGs generated are stored as adjacency lists in JSON files. This ensures a lightweight, language-agnostic universal format that facilitates efficient storage, management, update, and query. During agentic RCA, PRAXIS loads the PDG for each microservice under investigation at runtime.

Figure 2 shows a representative PDG of the Recommendation service from [31], comprising function- and statement-level hammock blocks.⁴ Exp denotes expression statements (a block of contiguous, straight-line statements without branching), whereas other nodes represent branching logic (e.g., if/else). Function-level blocks are explicitly labeled with function names (e.g., ListRecommendation()).

²To avoid context overflow, only the K most recent entries are collected. We set $K = 40$ for our evaluation, as empirical testing showed that increasing the value further does not significantly alter RCA accuracy.

³For brevity, we do not show all nodes/edges in the figure.

⁴We omit the full PDG for brevity, as the actual structure contains 44 hammock blocks.

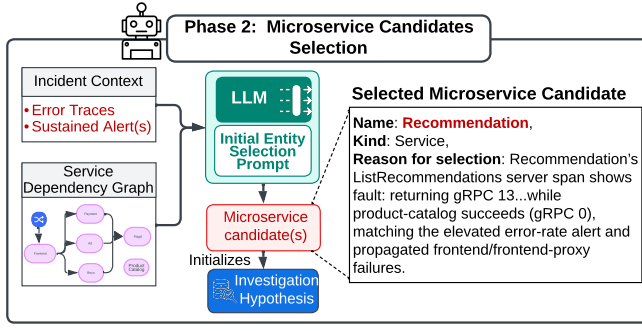


Fig. 3: PRAXIS Phase 2: Initial microservice candidate(s) selection.

B. Phase 2: Microservice Candidate(s) Selection

In Phase 2 (Figure 3), PRAXIS invokes an LLM to select an initial set of cloud *microservice candidates* potentially responsible for the incident to start the investigation process using the SDG and the incident context from Phase 1. PRAXIS prompts the LLM (denoted as \mathcal{M}) with ψ_{select} , conditioning the selection on the SDG $G_C = (V, E)$ and the incident context, which comprises active sustained alert(s) (A) and collected error traces (T). The LLM suggests a set of initial microservice candidates (up to N^5) from nodes in G_C , and outputs an initial *investigation narrative* I_0 describing the observed alerts, traces, and the reasons why they were selected. In addition, PRAXIS initializes an investigation queue Q to actively keep track of microservices that need to be investigated and initializes Q with those selected candidates: $Q \leftarrow \mathcal{M}(\psi_{select}(A, T, \lambda_V(G_C)))$.

Figure 3 shows an example microservice candidate selection, based on the sustained alert and error traces from Phase 1. LLM selects the *Recommendation service* as an initial candidate, noting that gRPC calls from the *Frontend service* exhibit gRPC 13 errors. These errors propagate upstream, manifesting as HTTP500 errors observed in the *Frontend service*.

The initial investigation narrative I_0 and the investigation queue Q serve as the starting point for PDG traversal and RCA decision-making in Phase 3.

C. Phase 3: RCA Decision-making

In Phase 3 (Figure 4), given the investigation queue Q and the initial investigation narrative I_0 from Phase 2, PRAXIS iteratively dequeues and investigates an entity e from the head of Q and determines its role (a root cause vs. a symptom) in the cloud incident.

For each dequeued entity $e_i \in Q$ (designated as the *focal entity*) at iteration i , PRAXIS first constructs the *observability context* c_i and retrieves the corresponding PDG G_P . It then retrieves the corresponding PDG G_P . Crucially, PRAXIS then employs an *LLM-driven PDG traversal* that traverses the entity (e_i)’s PDG (G_P) to construct an incident-centric program context C_P that explains the observed error symptoms from the perspective of entity code context. Given the observability context c_i and program context C_P of the focal entity, PRAXIS

uses the LLM to determine its role in the cloud incident as one of PRIMARY FAILURE (the root cause), SYMPTOM ONLY (a symptom), or UNRELATED. After finishing the investigation of the current entity, PRAXIS moves on to investigate the other LLM-selected microservices and the dependees according to the SDG G_C by adding them to the investigation queue Q . PRAXIS repeats this analysis on all entities in Q until Q is empty.

Specifically, this phase consists of the following steps:

(a) Observability context construction. PRAXIS first retrieves the focal entity e_i ’s observability data, comprising logs, metrics, and events, the SDG (G_C), and the focal entity’s PDG (G_P), built in Phase 1. PRAXIS additionally collects inter-service interactions (e.g., inbound/outbound calls) as indicated by the SDG and physical infrastructure attributes (e.g., cluster, node IDs) for each microservice-type entities. It also collects the current configuration status using Kubectl for ConfigMaps-type entities. PRAXIS structuralizes these collected data into a JSON representation at the time of incident investigation for the LLM to consume as *observability context* c_i , providing the most up-to-date runtime evidence to anchor the agentic program analysis and RCA reasoning.

(b) LLM-driven PDG traversal. Leveraging the observability context c_i and the graph G_P , the LLM agent operates in an iterative loop to traverse code paths defined by hammock blocks and code dependencies in the PDG. It analyzes how the underlying code logic aligns with the observed signals to pinpoint the root cause and explain the incident.

Initial hammock block (PDG node) selection. The first step to ensure that the PDG traversal begins from a semantically relevant point tied to the observed cloud incident is to identify the initial node b_0 in the PDG G_P as the starting point of the traversal. This node represents the code region most relevant to the observed symptom described in the entity’s observability context c_i (e.g., error descriptions, exception stack-trace, file name, and line numbers).

Given c_i and the PDG, we employ a language model \mathcal{M} conditioned on a prompt composition function ψ_{match} that encodes the runtime observability context c_i and the node attributes of the PDG λ_V (see §IV-A0b). Specifically, $\psi_{match}(c_i, \lambda_V)$ constructs a joint representation with:

- (1) observability data such as error logs, exception stack frames, error events, and metric anomalies;
- (2) PDG node metadata including the method names, corresponding code fragments, and file/line identifiers and string literals.

The language model \mathcal{M} then evaluates the correspondence between those two modalities and selects an initial hammock block node from G_P :

$$b_0 = \mathcal{M}(\psi_{match}(c_i, \lambda_V \in V(G_P)))$$

where $b_0 \in V(G_P)$ is a hammock block whose attributes (e.g., a string literal) correlate to the observed signals (e.g., a log entry). PRAXIS defaults to the hammock block corresponding to the entry-point (e.g., the main function) or request-handling methods (e.g., an API-handler function) of the microservice

⁵ N is a user-defined variable that we set to $N = 5$ for our experiments. Further increases of this value yielded no improvements to our results.

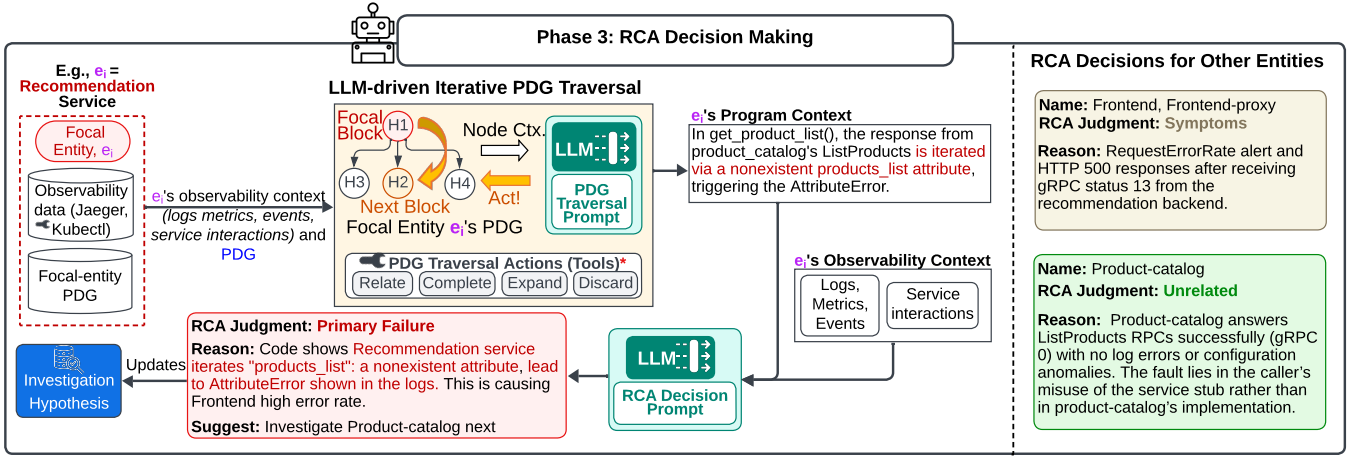


Fig. 4: PRAXIS Phase 3: RCA decision-making. This process is repeated for the next focal entity that is (a) a dependee of the current focal entity and/or (b) suggested by the LLM based on the focal entity’s RCA decision.

program when observability data are absent or insufficient due to the incident or when the matching is ambiguous (e.g., multiple matches).

PDG traversal. Once the starting hammock block b_0 (i.e., a node in PDG) has been identified, PRAXIS orchestrates the LLM’s iterative agentic traversal of the PDG (G_P) to construct program context C_P for in-depth RCA. Here, the program context C_P summarizes the microservice code paths that are likely related to the incident and explains the observed error symptoms from the perspective of this code path. As such, C_P provides rich, in-depth diagnostic context beyond symptom-level observability context for determining the microservice’s role in the incident.

We define this agentic process as a 4-tuple:

$$\mathcal{A} = \langle \mathcal{M}, \mathcal{T}, \mathcal{S}, G_P \rangle$$

- \mathcal{M} is the LLM used for reasoning and decision-making;
- \mathcal{T} is the tool-set used by \mathcal{M} to traverse over the PDG;
- \mathcal{S} is the agent’s state space;
- G_P is the PDG for microservice e_i that acts as a transition function according to the tool action.

The PDG traversal starts from the initial hammock-block node, $b_j = b_0$, which serves as the initial anchor in the PDG. At each PDG-traversal iteration j , we define the state as:

$$s_j = \langle b_j, B_{related}, c_i, H_j \rangle \in \mathcal{S}$$

where $b_j \in V(G_P)$ is the current hammock-block node under analysis; $B_{related}$ is the set of blocks in G_P related to b_j by control, data, or call dependencies ($B_{related} = \{b | (b_j, b_k) \in E(G_P)\}$); c_i is the current microservice’s observability context; and H_j is the past traversal history up to step j as PDG-traversal memory.

Conditioned on the current state s_j , the LLM \mathcal{M} produces a code-insight (ι_j) and the graph-traversal action (a_j) pair, i.e., $(a_j, \iota_j) = \mathcal{M}(\psi_\tau(s_j))$, where \mathcal{M} is the LLM executing the reasoning and policy selection. ψ_τ is the prompt composer that encodes the current state s_j into a structured form parametrized by a template τ . In particular, b_j and $B_{related}$ ’s corresponding code snippets and relations are fetched by ψ_τ . $a_j \in \mathcal{T}$ is

the next chosen action (mapped to our tools), and ι_j is the natural-language insight derived as the outcome of the current state/action. Notice that the LLM only consumes code context local to hammock blocks ($b_j, B_{related}$) for each traversal step, instead of large code files or codebases; this reduces reasoning context space and allows the LLM to focus on concise, accurate context relevant to the incident, as indicated by c_i .

The agent’s traversal action is implemented with a set of PDG traversal tools \mathcal{T} . Each tool in \mathcal{T} corresponds to a concrete, admissible traversal action on the PDG G_P . Table I provides a detailed summary of the above tools. When an inadmissible action (e.g., a non-existent block) is rejected by \mathcal{T} , PRAXIS prompts the LLM to regenerate a traversal action, subject to a predefined retry limit. Each action invocation updates the traversal history (H_{i+1}) and fetches the next node ($b_{j+1} \in G_P$) deterministically based on a_j via \mathcal{T} on G_P : $b_{j+1} = \mathcal{T}(G_P; a_j)$, $H_{j+1} = H_j \cup \{b_j, \iota_j, a_j\}$; we can then construct s_{j+1} accordingly for the next iteration.

Figure 5 illustrates a traversal step wherein the LLM selects the Relate action to focus on Block 1 (get_product_list function) to further investigate the observed AttributeError, as the LLM reasons that the observed AttributeError is caught within the current focal block (try-catch statement) and likely originated in get_product_list.

The traversal terminates when one of the actions, COMPLETE or DISCARD, is produced, when all the nodes are exhausted, or when the user-defined budget (e.g., max number of blocks) is reached. Upon completion, the agent updates its memory state H by committing the final traversal record, yielding the complete traversal history H_T (assuming T traversal steps in total). Notice that the visited code blocks ($\{b_0, b_1, \dots, b_T\}$) encompassed in H_T form a code dependency path admitted by control, data, and call dependencies. Then, the LLM uses a prompt ψ_{syn} to combine traversal history and observability context, producing the final program context $C_P(e_i)$ for microservice e_i : $C_P(e_i) = \mathcal{M}(\psi_{syn}(H_T, c_i))$. Here, C_P highlights code regions, dependencies, and explanations, which

TABLE I: PDG traversal tools available to the agent during graph-based program analysis.

Tool	PDG Operation	Description	Effect on Reasoning
Expand	$\text{parent}(b_i)$	Moves to the immediate parent or dominator node.	Broaden to examine higher-level hammock blocks or callsites.
Relate	$\Gamma(b_i)$	Visits neighboring nodes linked by call, control, or data dependencies.	Explores adjacent code paths to collect supporting or refuting evidence.
Complete	—	Terminates traversal and triggers synthesis of program context C_P .	Consolidates and finalizes the code-level hypothesis.
Discard	—	Terminates traversal without using current findings.	Prunes irrelevant or low-confidence trajectories.

The traversal tool-set $\mathcal{T} = \{\text{Expand}, \text{Relate}, \text{Complete}, \text{Discard}\}$ defines the discrete action space of the agent. Each action is implemented as a callable operation on the versioned PDG stored in the Neo4j-like graph database.

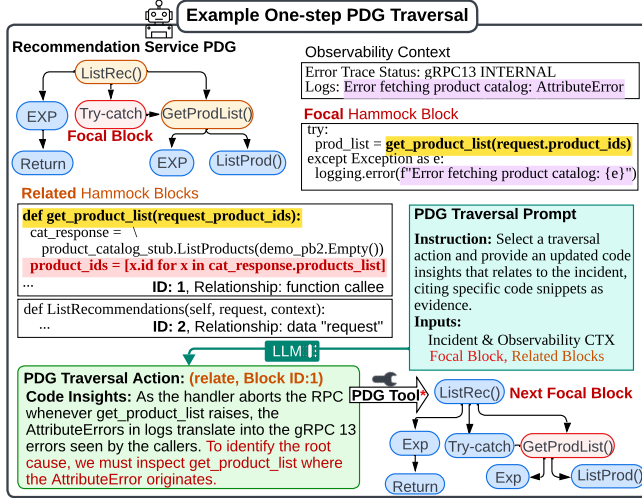


Fig. 5: Example LLM-driven PDG traversal.

link error signals in the observability data with program evidence (code snippets and dependency flows) that might explain the incident.

(c) **Entity role judgment and queue update.** The final stage in this phase is entity role judgment and investigation queue update, in which PRAXIS provides a diagnostic judgment on the entity e_i 's role in the incident and an admissible explanation with evidence, and updates the investigation queue accordingly.

Entity role judgment. After the program context for the entity e_i has been synthesized, PRAXIS determines the role of the current entity e_i in the incident: whether e_i is the root cause (primary cause of failure), a symptom, or unrelated. The role is inferred by a language model \mathcal{M} conditioned on a prompt ψ_j that composes observability (c_i) and program context (C_P) into a reasoning prompt for the LLM \mathcal{M} , i.e., $J = \mathcal{M}(\psi_j(c_i, C_P))$, where J is one of $\{\text{PRIMARY FAILURE}, \text{SYMPTOM ONLY}, \text{or UNRELATED}\}$. The model returns both the categorical judgment J and its natural language reasoning (I_{e_i}) with evidence grounded in both observability and program context (c_i and C_P). I_{e_i} is then appended to the global investigation narrative $I = I \cup I_{e_i}$ used in subsequent investigation.

Investigation queue update. The entity investigation queue Q is then expanded to include new entities that are: (a) dependees of the current focal entity, and/or (b) suggested by the LLM based on the focal entity's RCA decision. For

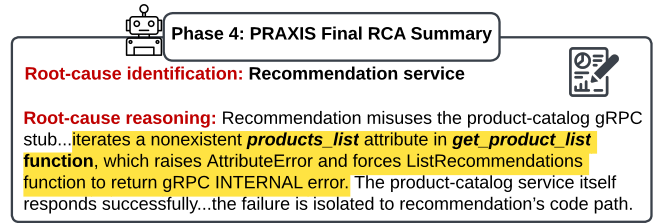


Fig. 6: PRAXIS Phase 4: Final RCA summary.

(a), PRAXIS enqueues all unvisited dependees (i.e., cloud entities on which e_i depends) according to the SDG G_C , denoted as $Q_{G_C} = G_C.\text{getDependees}(e_i)$. For (b), PRAXIS prompts the LLM \mathcal{M} using the entity-queueing prompt ψ_Q to identify up to k additional entities⁶ from G_C . This selection is based on the judgment J , the observability context c_i , the program context C_P , and the nodes in the SDG G_C , such that $Q_{M_Q} = \mathcal{M}(\psi_Q(J, c_i, C_P, G_C))$. Finally, the queue is updated: $Q = Q \cup Q_{M_Q} \cup Q_{G_C}$. Mechanism (b) is crucial as it allows the LLM to investigate entities in G_C that surface from the program context C_P despite having partial or missing observability data (due to insufficient coverage or the incident itself). Our evaluation confirms that this capability helps diagnose entities that do not emit observability data (e.g., a ConfigMap) or have failed silently.

Figure 4 depicts the investigation of the Recommendation service (selected in Phase 2, Figure 3), which was classified as a PRIMARY FAILURE based on its program (C_P) and observability (c_i) contexts as well as subsequent RCA judgments for the Frontend, Frontend-proxy, and Product-catalog services.

PRAXIS **repeats** this phase (Phase 3) for the next entity e_{i+1} at the head of the updated queue Q . By cross-traversing between the SDG and PDG, PRAXIS can resolve cloud incidents that require multiple hops to root-cause the incident while maintaining a coherent RCA summary via a consistent stream of investigation narrative I —a feature that is unobtainable by simply combining independent agents [16], [18], [32], [33]. Critically, leveraging code-level insights to bypass gaps in the SDG, PRAXIS can traverse across missing links (e.g, error traces, logs) in observability data, as shown by the Cross-SDG-PDG traversal example in §III.

Moreover, by iteratively traversing the PDG node-by-node, PRAXIS progressively refines the RCA scope—transitioning from broader service-level observability signals to a more focused analysis of specific code regions for each focal entity. Consequently, at each step, the LLM is strictly exposed to the local context of the current graph node rather than multiple microservices or codebases/code files. This isolation of unrelated information (other node contexts) improves context efficiency, reduces token consumption, and mitigates potential context overflow, allowing PRAXIS to scale effectively to large cloud applications and codebases.

⁶We set $k = 3$ in our implementation; however, we did not observe the LLM selecting more than two entities.

D. Phase 4: Final RCA Summary

After all entities in Q have been investigated, the LLM \mathcal{M} synthesizes a comprehensive RCA report using its accumulated investigation history I from Phase 3 with a prompt $\psi_{summary}$ to produce a diagnosis report D , i.e., $D = \mathcal{M}(\psi_{summary}(I))$. D identifies the primary failure entities (root-cause entities), root-cause reasoning, and fault propagation chain, while providing a justification for each entity’s diagnosis, citing evidence from the microservice code and observability data. This step consolidates the investigation and generates a structured, human-readable RCA report grounded in both observability and program-level reasoning.

Figure 6 presents an example final RCA report. PRAXIS correctly identifies the Recommendation service as the root cause, specifically attributing the failure to a schema mismatch (accessing non-existent fields), and suggests remediation. It also accurately classifies Frontend and Frontend-proxy as symptoms-only and Product-catalog as unrelated.

V. EXPERIMENT SETUP

This section first clarifies the problem and evaluation scope, and then presents the cloud incident scenarios and implementations, baselines, and metrics used for evaluation.

A. Problem and Evaluation Scope

We evaluate PRAXIS on application-level incidents, focusing on microservice codebases for which source code is available for analysis. Our approach is beneficial even under partial code availability, as reasoning over available code improves diagnostic accuracy (Section VI); when source code is unavailable, PRAXIS falls back to using only observability and incident contexts for RCA. Gains are naturally limited when no code is available (Section VI-B). PRAXIS’s scope is confined to incident diagnosis within the investigation/diagnosis phase of the cloud incident lifecycle [21], [34].

B. Cloud Incident Evaluation Scenarios

We developed the *Code-Cloud-RCA Benchmark* comprising 30 cloud incidents using [31], same cloud application used successfully in [20], supported by a standard monitoring stack [23]–[25], [28], [35]. These scenarios are distilled from root-cause types commonly reported in production studies [3], [10]–[13], [36] and real-world incidents [11], [37]. Table II enumerates the scenario templates, fault mechanisms, expected symptoms, and reference to real-world incidents; the rightmost column (#) records the number of scenarios per template. As with any benchmark, comprehensive coverage cannot be guaranteed, and by providing this benchmark, we invite the broader community to contribute to and expand its scope. Scenarios driven by the same template vary in timing (startup vs. serving), observability (stack traces vs. error logs vs. error codes), failure modes (stalls vs. rapid retries), or configurations, and are annotated with ground-truth root-cause microservice and reasoning. We will submit these artifacts for evaluation and open-source the benchmark.

TABLE II: Incident scenario descriptions and real-world reference. Deployment/resource cases are included as negative examples to highlight PRAXIS’s limitations.

Scenario description	Mechanism / How simulated	Typical symptoms (Real-world incidents)	#
Data schema mismatch/incompatibility between services	Access a non-existent field (products_list) in a protobuf response from another microservice.	Unhandled exception; 5xx bursts; request failures. (Monzo 2017 outage [4]; report [3], [11], [13]).	4
Improper handling of external dependency failures	Upstream DB/service hangs or returns empty results; dependent service stalls without timeout or enters rapid retries.	Latency spikes; retry storms; high error rate. (Discord 2023 outage [38]; report [3], [10], [12], [13]).	6
Internal logic bug	Invert an assertion or suboptimal implementation (e.g., an exponential-time LCS ranking algorithm).	Slowness/timeouts; intermittent crashes; incorrect results. (Cloudflare 2019 outage [39]; report [10], [12], [13], [36])	2
Resource label mismatch	Hardcoded, outdated label prevents discovery of intended DB/service.	Connection refused; startup failure; unavailability. (Reddit 2023 outage [5]; report [10], [11], [13])	2
Constant misconfiguration	Wrong env/DB constant (e.g., array length) distorts control flow.	Out-of-bounds access; crashes; error bursts. (CrowdStrike 2024 outage [40]; report [3])	2
Feature-flag ConfigMaps misconfiguration	Incorrect shared Flagd rules/config; effects depend on code paths and flag usage.	Crashes; pod terminations; CPU/memory pressure. (Spotify 2025 incident [41]; report [3], [13])	9
Deployment manifest error	Invalid image tag or replicas=0.	ImagePullBackOff; service unavailable. (Quryio 2020 outage [42]; report [3])	2
Resource-related fault	Chaos Mesh: CPU stress, node-level network outage, JVM corruption.	Saturation; packet loss; node/pod failures. (Multiple cases in [11])	3

C. Baselines

We benchmarked PRAXIS against ReAct-style [43] RCA agents [14]:

SRE-Agent (baseline). ReAct-style SRE-Agent [14] that uses standard SRE tools to access Kubernetes API, traces, metrics, events, and microservices application logs.

SRE-Agent+CT (baseline+). Extends SRE-Agent with *code tools (CT)* for code retrieval, inspection, and summarization, adding code context to the baseline.

PRAXIS (ours). The proposed method, PRAXIS, employs LLM-driven reasoning and traversal over program dependence and service dependency graphs.

TABLE III: Evaluation result of baseline and PRAXIS.

LLM model	RCR Pass@1% \uparrow	RCI Pass@1% \uparrow
SRE-Agent		
gpt-oss-120b	2.68 \pm 1.32	8.72 \pm 2.31
deepseek-r1	5.48 \pm 1.88	20.44 \pm 3.34
o4-mini	9.86 \pm 2.50	22.54 \pm 3.50
mistral-medium-3.1	14.62 \pm 3.10	28.46 \pm 3.96
gpt-5	19.71 \pm 3.40	35.77 \pm 4.10
gpt-5-codex	5.37 \pm 1.85	13.42 \pm 2.79
SRE-Agent + Code Tools (CT)		
gpt-oss-120b	2.01 \pm 1.15	6.71 \pm 2.01
deepseek-r1	4.68 \pm 2.64	17.18 \pm 4.72
o4-mini	7.63 \pm 2.21	24.31 \pm 3.57
mistral-medium-3.1	16.15 \pm 3.22	27.69 \pm 3.93
gpt-5	25.55 \pm 3.73	36.50 \pm 4.11
gpt-5-codex	5.63 \pm 1.93	10.56 \pm 2.58
PRAXIS (Ours)		
gpt-oss-120b	48.28 \pm 4.15	71.03 \pm 3.77
deepseek-r1	37.50 \pm 4.74	57.69 \pm 4.84
o4-mini	54.16 \pm 4.15	70.14 \pm 3.81
mistral-medium-3.1	4.37 \pm 1.74	23.36 \pm 3.61
gpt-5	57.55 \pm 4.19	72.66 \pm 3.78
gpt-5-codex	61.54 \pm 4.27	73.85 \pm 3.85

Metrics: (i) **RCR Pass@1**: Pass@1 % score for root cause reasoning; (ii) **RCI Pass@1**: root cause identification accuracy. Best-performing agent+LLM model is shown in **bold**, and the second-best is underlined. Higher is better.

D. Evaluation Metrics

We evaluated RCA effectiveness with respect to the below metrics following the same definitions as [14]:

Root cause reasoning (RCR) Pass@1 (%) : Pass@1 accuracy of the agent’s RCA reasoning (explanation by identifying statement(s), function(s), or configuration(s) at fault) compare against ground truth, following *Pass@K* [44] with $K = 1$.

Root cause identification (RCI) Pass@1 (%) : The percentage of instances where the identified faulty microservice(s) exactly match the ground truth.

We also report RCA efficiency via **MTTD** (mean time to diagnosis) and **ATC** (average token consumption).

E. PRAXIS Implementation

PRAXIS is implemented in Python 3.12 using the LangGraph agentic framework [45]. PRAXIS supports PDG construction for microservices written in Python and Java, a scope we chose based on current toolchain availability and the popularity of these languages [46]. For evaluation purposes, all faults implemented reside in codebases available for analysis and supported by PRAXIS. We will submit our artifacts for evaluation and open-source the implementation.

VI. EVALUATION RESULTS

We answer the following research questions (RQs):

RQ-1 (§VI-A): How accurate is PRAXIS compared to baseline agents for cloud incident RCA?

RQ-2 (§VI-B): How does incident-centric program context via PDG reasoning contribute to PRAXIS’s improvement?

RQ-3 (§VI-C): What are the diagnosis overheads of incorporating program context in cloud RCA?

A. Baseline Comparison (RQ1)

For RQ-1, we evaluated PRAXIS by comparing it against the current state of the art, i.e., the SRE-Agent [14], a ReAct-style RCA agent with default tools, and an extended SRE-Agent with code retrieval and summarization tools (denoted by SRE-Agent+CT) to study whether code context can improve on the baseline performance.

Evaluation setup. We evaluated the baselines and PRAXIS across six different LLMs: o4-mini, gpt-5, gpt-5-codex, mistral-medium-3.1, deepseek-r1, and gpt-oss-120b. For statistical robustness, we repeated each (LLM, scenario) experiment five times with different random seeds, totaling 2,700 trajectories.

Overall results. As shown in Table III, PRAXIS consistently performed better than SRE-Agent and SRE-Agent+CT across the LLMs that were evaluated, both on root-cause reasoning (RCR) accuracy and root-cause identification (RCI) accuracy. PRAXIS’s RCA reasoning accuracy correlates strongly with root-cause identification accuracy, reflecting how human SREs rely on accurate fault pinpointing for effective root-cause analysis.

For ReAct-style SRE agent baselines, RCA accuracy is tightly coupled to tool-calling: models with stronger tool use (mistral-medium-3.1, gpt-5) achieve higher RCA accuracy, whereas strong reasoning models not tuned for tool usage (e.g., o4-mini, deepseek-r1) underperform due to inconsistent tool calls. These inconsistencies cause them to invoke incorrect tools, pass incorrect parameters, or skip necessary tools, leading investigations to end with symptom-level explanations (e.g., error traces) rather than true root causes. The gap between gpt-5 and gpt-5-codex within the same model family manifests this issue: gpt-5-codex, tuned primarily for code-centric tasks and tools, attains lower RCA accuracy than gpt-5, which is tuned for more general tool-calling and thus generalizes better to both SRE and code tools required for RCA.

For PRAXIS, RCA accuracy correlates more closely with the model’s reasoning capabilities: models with stronger reasoning (gpt-5, gpt-5-codex, o4-mini) exhibit higher RCA accuracy overall. Moreover, we speculate that the stronger performance of gpt-5-codex compared to gpt-5 stems from its superior code-understanding capabilities (as demonstrated on [47]), which better support correlating code context and program behavior with the incident. The low accuracy of mistral-medium-3.1 is primarily due to its failure to select appropriate initial candidates and its inability to follow output-format instructions, which frequently led to output parsing errors.

Why did baselines underperform? SRE-Agent underperformed because it lacks code visibility, which is essential for diagnosing code-related scenarios. Adding code tools (SRE-Agent+CT) improves accuracy with gpt-5 but yields only marginal gains for other LLMs. This is not because code tools are unhelpful, but because the baseline agents’ investigation decision-making remains unstructured and unguided. Baseline ReAct-style agents make diagnosis decisions (as additional tool-calls or termination) primarily from the most recent tool-call states and observations, without an explicit representation

of or planning over the underlying dependency graphs, making their RCA accuracy heavily dependent on the model’s tool-calling capabilities. As a result, even with both code and SRE tools, models not tuned for general tool use (e.g., o4-mini, gpt-5-codex) tend to exhibit two failure modes: (1) *premature closure*: once local evidence appears to *explain* the alerts (e.g., an *HTTP 500* handler or related error traces), they terminate the investigation without diving deeper; and (2) *tool-usage fragility*: invoking incorrect tools or supplying incorrect parameters [48], [49]. Additionally, without explicit awareness or external imposition of the microservice or program dependencies, these baselines had neither a mechanism nor an obligation to traverse the multi-hop dependency chain (which in our scenarios often involved 7–10 hops across different microservices and their hammock blocks) in which the true root-causes were hinted or resided.

Notably, even with explicit instructions in the prompt to invoke code tools, SRE-Agent+CT with gpt-5, the best-performing model, invoked code tools in only 32% of runs where code analysis was required for RCA. This under-use of required tools led to lower RCA accuracy and inconsistent execution trajectories, reinforcing the baseline agent failure modes described above. In contrast, PRAXIS treats service and code-level dependencies as first-class as it constrains the LLM’s reasoning onto the dependency paths in PDG and systematically expands each graph node’s neighborhood with admissible graph traversal actions, enforcing iterative context gathering and reasoning reconciliation. This graph-aware reasoning prevents early stopping on symptomatic context and steers the investigation to the upstream root cause in code, achieving in-depth RCA.

B. Ablation Study (RQ2)

For this RQ, we conducted an ablation study to assess the impact of PRAXIS’s core components on RCA effectiveness by evaluating the following PRAXIS variants.

PRAXIS (Obs. Ctx.): This variant disables PDG-traversal and program context (C_P), so only the incident context and observability context (c_i) are used in the RCA decision in §IV-C. This experiment characterized the performance gains resulting from the use of program context.

PRAXIS (Raw Code): The Raw Code variant skips PDG construction (§IV-A0b) and LLM-driven PDG traversal (§IV-C) when constructing C_P and instead uses an LLM with a modified ψ_{syn} prompt (§IV-C) to consolidate and generate program context directly from aggregated raw code files. We limited the raw code to 800k characters to prevent context overflow.

Evaluation setup. We evaluated these PRAXIS variants using the best-performing LLM for PRAXIS—gpt-5-codex. For statistical robustness, we repeated each (variant, scenario) experiment five times with distinct random seeds, yielding an additional 300 trajectories.

Ablation results. Table IV shows that augmenting the observability context c_i with program context C_P (PDG construction + LLM-guided traversal) is the primary driver of RCA effectiveness. Relative to PRAXIS (Raw Code), PRAXIS

TABLE IV: Ablation study results on all scenario instances.

Agent Variant	Overall RCA Accuracy	
	RCR Pass@1%↑	RCI Pass@1%↑
PRAXIS (Obs. Ctx.)	12.93 ± 2.77	41.50 ± 4.06
PRAXIS (Raw Code)	32.65 ± 3.87	59.18 ± 4.05
PRAXIS (Ours)	61.54 ± 4.27	73.85 ± 3.85
<i>Data Schema Mismatch</i>		
PRAXIS (Obs. Ctx.)	40.0 ± 14.14	100.0 ± 0.0
PRAXIS (Raw Code)	25.0 ± 18.97	85.0 ± 14.14
PRAXIS (Ours)	70.0 ± 8.94	95.0 ± 8.93
<i>Improper Ext. Failure Handling</i>		
PRAXIS (Obs. Ctx.)	10.0 ± 11.54	33.3 ± 1.6
PRAXIS (Raw Code)	36.67 ± 20.0	43.33 ± 19.32
PRAXIS (Ours)	85.83 ± 12.57	86.0 ± 12.60
<i>Internal Logic Bug</i>		
PRAXIS (Obs. Ctx.)	20.0 ± 15.49	100.0 ± 0.0
PRAXIS (Raw Code)	50.0 ± 17.89	90.0 ± 12.65
PRAXIS (Ours)	80.0 ± 17.89	100.0 ± 0.0
<i>Resource Label Mismatch</i>		
PRAXIS (Obs. Ctx.)	30.0 ± 15.4	100.0 ± 0.0
PRAXIS (Raw Code)	40.0 ± 21.91	100.0 ± 0.00
PRAXIS (Ours)	80.0 ± 15.5	100.0 ± 0.0
<i>Constant Misconfiguration</i>		
PRAXIS (Obs. Ctx.)	0.0 ± 0.0	80.0 ± 15.0
PRAXIS (Raw Code)	20.0 ± 17.89	90.0 ± 12.65
PRAXIS (Ours)	90.0 ± 13.0	100.0 ± 0.0
<i>Feature-flag ConfigMaps Misconf.</i>		
PRAXIS (Obs. Ctx.)	0.0 ± 0.0	0.0 ± 0.0
PRAXIS (Raw Code)	45.56 ± 19.71	54.44 ± 19.71
PRAXIS (Ours)	62.96 ± 16.67	65.74 ± 18.16

We used the same RCA accuracy metrics as in Table III.

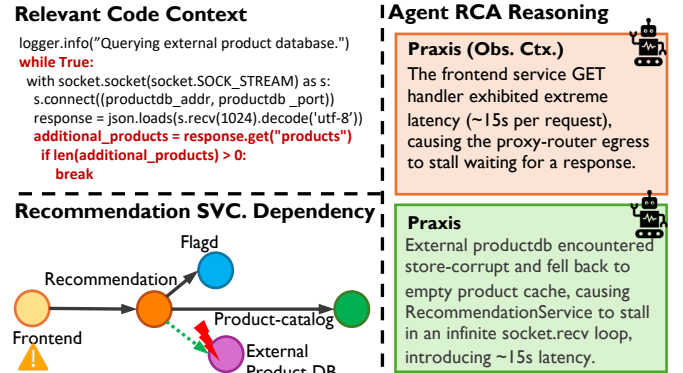


Fig. 7: RCA reasoning of PRAXIS (Obs. Ctx.) and PRAXIS. Nodes are microservices; solid arrows are dependencies; the green dotted arrow is a dependency with missing traces and had to be derived from program context.

improves overall RCR Pass@1 by 28.8 percentage points, from 32.7% to 61.5% (an 88.5% improvement), and RCI Pass@1 by 14.7 percentage points, from 59.2% to 73.9% (a 24.8% improvement). Against PRAXIS (Obs. Ctx.), the gains are larger, at 48.6 percentage points and 32.4 percentage points for RCR Pass@1 and RCI Pass@1, respectively.

Why do program context and LLM-driven PDG help?

Similar to the SRE-Agent baseline, PRAXIS without program context (PRAXIS (Obs. Ctx.)) failed to identify root causes within, or hinted by, the internal code logic, resulting in superficial symptom-level RCA. Although the PRAXIS variant without PDG (PRAXIS (Raw Code)) retains service-level dependency awareness, the absence of PDG-guided diagnosis halved its

accuracy compared to that of the full approach. Lacking explicit awareness of program-level dependencies, PRAXIS (Raw Code) cannot effectively focus its reasoning on code regions relevant to the incident. Instead, it “fixated” on ostensibly faulty regions—code that appears erroneous on the surface (e.g., manually thrown exceptions)—that are not pertinent to the observed failure. With code context exceeding 200k tokens at times, PRAXIS (Raw Code) exhibited *needle in a haystack* [50] and *context rot* [51] phenomena, leading to degraded RCA accuracy. These findings confirm that PDG-guided diagnosis is essential: it enforces the alignment of observability data with concise, accurate code context structurally presented to the LLM, grounding the RCA in relevant code paths and code regions to yield the observed performance gains.

Illustration. We illustrate the RCA reasoning specificity improvement using an “improper handling of external dependency failure” scenario. Here, a degraded external database returned empty responses, triggering a silent retry loop in the Recommendation service that manifested solely as high latency, without explicit error logs. As shown in Figure 7, PRAXIS without program context failed to detect this behavioral pattern, wrongly identifying the high latency, a symptom, as the root cause. Conversely, utilization of program context enabled PRAXIS to identify the retry logic and uncover the database dependency, correctly isolating the underlying storage issue (storage corruption → empty product list) as the true root cause.

Per-scenario trends. PRAXIS’s improvements hold across most scenario types. For example, for *Constant Misconfiguration*, PRAXIS attained 90% RCR and 100% RCI while other agents achieved around 0%–20% RCR. A minor regression appeared in *Data Schema Mismatch* (RCI Pass@1 100.0% → 95.0%), likely because error signals in logs occasionally allow the observability-only variant (PRAXIS (Obs. Ctx.)) to correctly identify the faulty microservice without code analysis, although it is unable to arrive at the correct root cause. *Feature-flag ConfigMaps misconfiguration* scenarios remain challenging (RCI ≈ 66%), likely due to insufficient observability data for PRAXIS to exploit during the PDG-traversal and RCA decision-making.

C. Diagnosis Overheads (RQ3)

For this RQ, we evaluated the RCA overheads of SRE-Agent baselines, PRAXIS, PRAXIS (Obs. Ctx.), and PRAXIS (Raw Code) across all scenarios and using the best-performing LLMs: gpt-5 for SRE agent baselines, and gpt-5-codex for PRAXIS.

Evaluation setup. To account for differences in RCA reasoning accuracy, we normalized both MTTC and ATC by RCR Pass@1% to assess diagnosis efficiency: *Normalized metric* = $\frac{MTTC \text{ or } ATC}{RCR \text{ Pass@1\%}}$. The resulting normalized MTTC (i.e., mean time to diagnosis or MTTD) and normalized ATC (effective ATC) reflect time and token costs per successful diagnosis.

Table V shows that, when accounting for RCA accuracy, PRAXIS reduces MTTD by up to 24.8%⁷ relative to SRE-Agent

TABLE V: Diagnosis overheads across all scenario instances.

	MTTC↓	ATC↓	MTTD↓	Eff. ATC↓
SRE-Agent	346.81	123.06k	1,850.87	624.35k
SRE-Agent+CT	500.84	140.01k	1,960.23	547.98k
PRAXIS (Obs. Ctx.)	1,321.02	75.59k	10,475.97	599.44k
PRAXIS (Raw Code)	838.44	329.53k	2,567.96	1,009.28k
PRAXIS (Ours)	907.43	<u>102.44k</u>	1,474.54	166.46k

Metrics: (i) **MTTC** = mean time to completion in seconds; (ii) **ATC** = average token consumptions in tokens; (iii) **MTTD** = mean time to diagnosis; (iv) **Eff. ATC** = effective ATC. Best-performing variant is shown in **bold**; second-best is underlined. Lower is better.

baselines. Moreover, compared to PRAXIS, the SRE baselines consume up to 3.8× as many tokens per successful diagnosis, indicating substantially lower token efficiency.

When we compare PRAXIS with its ablated variants (PRAXIS (Raw Code)) and PRAXIS (Obs. Ctx.), construction of program context via LLM-driven PDG traversal reduced MTTD and effective ATC by up to 85.9% and 83.5%, respectively, highlighting their significant contributions to efficient RCA. Notably, LLM-driven PDG traversal resulted in a 6.1× reduction in ATC compared to that of supplying raw code as plain text in prompt (as in [19], [52]). PRAXIS’s MTTD of 1,474 seconds is substantially lower than that of manual RCA, which can take several hours for incidents with comparable root causes.

D. Limitations and Future Work

Scenarios with weak observability. PRAXIS’s effectiveness is contingent on the availability and quality of observability data to anchor its PDG traversal. Sparse traces, logs, metrics, or events can limit PRAXIS’s ability to accurately align runtime error signals with corresponding dependency paths to traverse. This limitation is most apparent for *Deployment Manifest Error* and *Resource-related Fault* incidents, where PRAXIS achieves near-zero accuracy (omitted from Table IV). PRAXIS tends to underperform in these cases because the fault often lies in the deployment manifest or third-party services, offering no direct observable signal to anchor RCA decision-making. Consequently, PRAXIS tends to falsely attribute the incident to healthy code paths, leading to false positives. While collecting exhaustive observability data could mitigate this, it would significantly incur production overheads.

Graph representation. PRAXIS’s effectiveness relies on the correctness and completeness of the dependency graphs. Dependency graphs that are incorrect or incomplete (e.g., an outdated PDG, or a missing microservice in SDG) hinder PRAXIS’s ability to localize the root cause. Moreover, PRAXIS is likely sensitive to the granularity of the node. For example, including large code context (module-level hammock block) can reduce diagnostic specificity, while a fine-grained representation (statement-level hammock block) risks missing broader context beneficial to RCA.

Code availability and static code analysis. PRAXIS’s gains from PDG traversal are naturally limited if microservice code is unavailable for graph construction and it must rely solely on observability data for diagnosis. Conversely, conditioning too strongly on static code context risks unintended bias, where PRAXIS may mistakenly attribute faults to code blocks when the incident actually stems from external factors (e.g., deployment

⁷Includes LLM backend response times.

or resources). This risk can be mitigated by incorporating runtime instrumentation to confirm whether implicated code paths were indeed executed at the time of the incident.

Future Work. Future iterations of PRAXIS will be extended to platform- and infrastructure-level incidents. We also plan to integrate *dynamic program analysis*—incorporating runtime tracing, heap snapshots, and dynamic slicing—to ground static analysis in verifiable runtime behavior, enabling more comprehensive and precise RCA.

VII. RELATED WORK

Agentic approach for cloud incident RCA. Recent agentic RCA approaches [14], [16]–[18], [20] adopted the ReAct paradigm [43] to analyze observability data but lack structured reasoning workflow and program context, limiting their effectiveness on software and misconfiguration faults. The prior approaches that include program/code context [15], [19] inline code in plain-text prompts without explicitly imposing the inherent code structure, as they do not employ a PDG-guided reasoning process. PRAXIS advances beyond those efforts by performing LLM-driven reasoning over service dependency and program dependence graphs, unifying incident, observability, cloud, and program context for scalable, end-to-end RCA.

AI/ML for specific RCA workflow automation. AI/ML techniques have long supported incident RCA through specialized models for anomaly detection, fault localization, and diagnosis [27], [53]–[57]. Recent work has employed LLMs for incident querying, understanding, and classification [52], [58]–[63], typically leveraging prior knowledge (e.g., TSGs, SOPs) and requiring SRE supervision. PRAXIS performs automated RCA end-to-end, and those methods can be considered complementary to it.

LLM for graph reasoning and traversal. LLM-driven graph reasoning/traversal is an emerging field [64] that can be applied to knowledge retrieval, question-answering [65]–[68], code search and localization [69], and execution path reconstruction [70]. Though graph models have been established in systems/AIOps [71], LLM-driven graph reasoning in this domain is still underexplored, and we have demonstrated its potential through PRAXIS.

VIII. CONCLUSION

This paper proposes PRAXIS, an agentic approach that reasons over microservice and program dependency graphs for a comprehensive, in-depth root-cause analysis. Our evaluation of PRAXIS on 30 scenarios that span software, configuration, deployment, and resource failures demonstrates that PRAXIS achieves up to $3.1\times$ better root-cause reasoning accuracy, $2.1\times$ higher root-cause identification accuracy, and a $3.8\times$ reduction in token consumption compared to state-of-the-art agentic baselines.

ACKNOWLEDGMENT

We thank R. Arora, B. Bhavya, N. Zheutlin, P. T. Isaza, J. Ahn, A. Paradkar, L. Shwartz, R. K. Kottapalli, A. D. Angelis, A. Patke, P. Cao, Z. Zheng, and J. Applequist for technical input

and feedback on early drafts of this work, and H. C. Fairrow, S. Weick, K. Atchley, Y. Deng, R. Pavuluri, M. Vukovic, X. Liu, D. Sow, and N. Fuller for administrative support. This work is supported by the IBM-Illinois Discovery Accelerator Institute (IIDAI). Any opinions expressed here are those of the authors and do not necessarily reflect the views of IBM.

REFERENCES

- [1] New Relic, Inc., “New Relic study reveals businesses face an annual median cost of \$76 million from high-impact IT outages,” Sep. 2025, press release. [Online]. Available: <https://newrelic.com/press-release/20250917>
- [2] —, “2025 observability forecast report,” 2025, report. [Online]. Available: <https://newrelic.com/sites/default/files/2025-09/new-relic-2025-observability-forecast-report.pdf>
- [3] S. Ghosh, M. Shetty, C. Bansal, and S. Nath, “How to fight production incidents? An empirical study on a large-scale cloud service,” in *Proceedings of the 13th Symposium on Cloud Computing*, ser. SoCC ’22. New York, NY, USA: Association for Computing Machinery, 2022, pp. 126–141. [Online]. Available: <https://doi.org/10.1145/3542929.3563482>
- [4] Monzo-engineer, “RESOLVED: Current account payments may fail: Major outage 27/10/2017,” Oct. 2017, Monzo Community Forum. Accessed 2025-10-20. [Online]. Available: <https://community.monzo.com/t/resolved-current-account-payments-may-fail-major-outage-27-10-2017/26296/95>
- [5] Reddit-engineer, “You broke Reddit: The Pi-Day outage,” Mar. 2023, Reddit Engineering Blog. Accessed: 2025-10-09. [Online]. Available: https://www.reddit.com/r/RedditEng/comments/11xx5o0/you_broke_reddit_the_piday_outage/
- [6] Amazon Web Services. (2025) Summary of the Amazon DynamoDB service disruption in the Northern Virginia (US-EAST-1) region. AWS. Post-incident summary of the Oct 19–20, 2025 US-EAST-1 disruption. [Online]. Available: <https://aws.amazon.com/message/101925/>
- [7] M. Prince, “Cloudflare outage on November 18, 2025,” <https://blog.cloudflare.com/18-november-2025-outage/>, Nov. 2025, accessed: 2025-11-20.
- [8] R. Johnson, D. Pearson, and K. Pingali, “The program structure tree: Computing control regions in linear time,” in *Proceedings of the ACM SIGPLAN 1994 Conference on Programming Language Design and Implementation*, ser. PLDI ’94. New York, NY, USA: Association for Computing Machinery, 1994, pp. 171–185. [Online]. Available: <https://doi.org/10.1145/178243.178258>
- [9] F. Zhang and E. H. D’Hollander, “Using hammock graphs to structure programs,” *IEEE Trans. Softw. Eng.*, vol. 30, no. 4, pp. 231–245, Apr. 2004. [Online]. Available: <https://doi.org/10.1109/TSE.2004.1274043>
- [10] H. S. Gunawi *et al.*, “Cloud bug study (cbs) database,” <http://ucare.cs.uchicago.edu/projects/cbs/>, UCARE Research Group, University of Chicago, 2014, accessed: 2025-06-01.
- [11] H. Jacobs, “Kubernetes failure stories,” <https://codeberg.org/hjacobs/kubernetes-failure-stories>, 2023, accessed: 2025-10-07.
- [12] H. S. Gunawi, M. Hao, T. Leesatapornwongsa, T. Patana-anake, T. Do, J. Adityatama, K. J. Eliazar, A. Laksono, J. F. Lukman, V. Martin, and A. D. Satria, “What bugs live in the cloud? A study of 3000+ issues in cloud systems,” in *Proceedings of the ACM Symposium on Cloud Computing*, ser. SOCC ’14. New York, NY, USA: Association for Computing Machinery, 2014, pp. 1–14. [Online]. Available: <https://doi.org/10.1145/2670979.2670986>
- [13] H. Liu, S. Lu, M. Musuvathi, and S. Nath, “What bugs cause production cloud incidents?” in *Proceedings of the Workshop on Hot Topics in Operating Systems*, ser. HotOS ’19. New York, NY, USA: Association for Computing Machinery, 2019, pp. 155–162. [Online]. Available: <https://doi.org/10.1145/3317550.3321438>
- [14] S. Jha, R. R. Arora, Y. Watanabe, T. Yanagawa, Y. Chen, J. Clark, B. Bhavya, M. Verma, H. Kumar, H. Kitahara, N. Zheutlin, S. Takano, D. Pathak, F. George, X. Wu, B. O. Turkkkan, G. Vanloo, M. Nidd, T. Dai, O. Chatterjee, P. Gupta, S. Samanta, P. Aggarwal, R. Lee, J. wook Ahn, D. Kar, A. Paradkar, Y. Deng, P. Moogi, P. Mohapatra, N. Abe, C. Narayanaswami, T. Xu, L. R. Varshney, R. Mahindru, A. Sailer, L. Shwartz, D. Sow, N. C. M. Fuller, and R. Puri, “ITBench: Evaluating AI agents across diverse real-world IT automation tasks,”

- in *Forty-second International Conference on Machine Learning*, 2025. [Online]. Available: <https://openreview.net/forum?id=jP59rz1bZk>
- [15] Z. Wang, Z. Liu, Y. Zhang, A. Zhong, J. Wang, F. Yin, L. Fan, L. Wu, and Q. Wen, "RCAgent: Cloud root cause analysis by autonomous agents with tool-augmented large language models," in *Proceedings of the 33rd ACM International Conference on Information and Knowledge Management*, ser. CIKM '24. New York, NY, USA: Association for Computing Machinery, 2024, pp. 4966–4974. [Online]. Available: <https://doi.org/10.1145/3627673.3680016>
 - [16] Y. Chen, J. Pan, J. Clark, Y. Su, N. Zheutlin, B. Bhavya, R. Arora, Y. Deng, S. Jha, and T. Xu, "Stratus: A multi-agent system for autonomous reliability engineering of modern clouds," in *Proceedings of the 39th Conference on Neural Information Processing Systems (NeurIPS 2025)*, 2025, accepted; preprint available at arXiv:2506.02009. [Online]. Available: <https://arxiv.org/abs/2506.02009>
 - [17] D. Roy, X. Zhang, R. Bhaye, C. Bansal, P. Las-Casas, R. Fonseca, and S. Rajmohan, "Exploring LLM-based agents for root cause analysis," in *Companion Proceedings of the 32nd ACM International Conference on the Foundations of Software Engineering*, ser. FSE 2024. New York, NY, USA: Association for Computing Machinery, 2024, pp. 208–219. [Online]. Available: <https://doi.org/10.1145/3663529.3663841>
 - [18] J. Xu, Q. Zhang, Z. Zhong, S. He, C. Zhang, Q. Lin, D. Pei, P. He, D. Zhang, and Q. Zhang, "OpenRCA: Can large language models locate the root cause of software failures?" in *The Thirteenth International Conference on Learning Representations*, 2025. [Online]. Available: <https://openreview.net/forum?id=M4qNlZQYpd>
 - [19] Y. Li, Y. Wu, J. Liu, Z. Jiang, Z. Chen, G. Yu, and M. R. Lyu, "COCA: Generative root cause analysis for distributed systems with code knowledge," in *Proceedings of the 47th IEEE/ACM International Conference on Software Engineering (ICSE '25)*, 2025. [Online]. Available: <https://dl.acm.org/doi/10.1109/ICSE55347.2025.00234>
 - [20] Y. Chen, M. Shetty, G. Somashekar, M. Ma, Y. Simmhan, J. Mace, C. Bansal, R. Wang, and S. Rajmohan, "AIOpsLab: A holistic framework to evaluate AI agents for enabling autonomous clouds," in *Proceedings of MLSys '25*, 2025. [Online]. Available: <https://openreview.net/forum?id=3EXBLwGxtq>
 - [21] B. Beyer, C. Jones, J. Petoff, and N. R. Murphy, *Site Reliability Engineering: How Google Runs Production Systems*, 2016. [Online]. Available: <http://landing.google.com/sre/book.html>
 - [22] J. Ferrante, K. J. Ottenstein, and J. D. Warren, "The program dependence graph and its use in optimization," *ACM Trans. Program. Lang. Syst.*, vol. 9, no. 3, pp. 319–349, Jul. 1987. [Online]. Available: <https://doi.org/10.1145/24039.24041>
 - [23] Prometheus Authors, "Prometheus: Monitoring system & time series database," 2025, open-source systems monitoring and alerting toolkit. [Online]. Available: <https://prometheus.io/>
 - [24] Jaeger Project, "Jaeger: Open source, distributed tracing platform," 2025, originally open-sourced by Uber; CNCF project. [Online]. Available: <https://www.jaegertracing.io/>
 - [25] ClickHouse, Inc., "ClickHouse: Fast open-source OLAP DBMS," 2025, column-oriented database for real-time analytics. [Online]. Available: <https://clickhouse.com/>
 - [26] L. Wu, J. Tordsson, E. Elmroth, and O. Kao, "MicroRCA: Root cause localization of performance issues in microservices," in *NOMS 2020: 2020 IEEE/IFIP Network Operations and Management Symposium*, 2020, pp. 1–9. [Online]. Available: <https://doi.org/10.1109/NOMS47738.2020.9110353>
 - [27] Y. Gan, M. Liang, S. Dev, D. Lo, and C. Delimitrou, "Sage: Practical and scalable ML-driven performance debugging in microservices," in *Proceedings of the 26th ACM International Conference on Architectural Support for Programming Languages and Operating Systems*, ser. ASPLOS '21. New York, NY, USA: Association for Computing Machinery, 2021, pp. 135–151. [Online]. Available: <https://doi.org/10.1145/3445814.3446700>
 - [28] Datadog, "Datadog cloud monitoring platform," <https://www.datadoghq.com/>, 2025, accessed: 2025-06-01.
 - [29] M. Brunsfeld, A. Qureshi, A. Hlynyskiy, ObserverOfTime, W. Lillis, J. Vera, dundargoc, P. Turnbull, T. Clem, D. Creager, A. Helwer, R. Rix, D. Kavolis, C. Clason, M. Davis, R. Bruins, A. Delpeuch, Ika, A. Ya, T.-A. Nguyen, bfiredl, S. Brunk, M. Massicotte, N. Hasabnis, J. McCoy, M. Dong, S. Moelius, S. Kalt, and Kolja, "tree-sitter/tree-sitter: v0.25.10," September 2025, software; MIT License. [Online]. Available: <https://doi.org/10.5281/zenodo.17180150>
 - [30] R. Krishna, R. Pan, S. Sinha, S. Tamilselvam, R. Pavuluri, and M. Vukovic, "Codellm-Devkit: A framework for contextualizing code LLMs with program analysis insights," in *Proceedings of the 33rd ACM International Conference on the Foundations of Software Engineering*, ser. FSE Companion '25. New York, NY, USA: Association for Computing Machinery, 2025, pp. 308–318. [Online]. Available: <https://doi.org/10.1145/3696630.3728555>
 - [31] OpenTelemetry authors, "OpenTelemetry demo: Astronomy shop microservices," <https://github.com/open-telemetry/opentelemetry-demo>, 2025, microservice-based distributed system illustrating OpenTelemetry in a near real-world environment. Accessed: 2025-11-28.
 - [32] T. Ahmed, S. Ghosh, C. Bansal, T. Zimmermann, X. Zhang, and S. Rajmohan, "Recommending root-cause and mitigation steps for cloud incidents using large language models," in *Proceedings of the 45th International Conference on Software Engineering*, ser. ICSE '23. IEEE Press, 2023, pp. 1737–1749. [Online]. Available: <https://doi.org/10.1109/ICSE48619.2023.00149>
 - [33] J. Yang, C. E. Jimenez, A. Wettig, K. Lieret, S. Yao, K. Narasimhan, and O. Press, "Swe-agent: agent-computer interfaces enable automated software engineering," in *Proceedings of the 38th International Conference on Neural Information Processing Systems*, ser. NIPS '24. Red Hook, NY, USA: Curran Associates Inc., 2024.
 - [34] Google Cloud, "Lifecycle of an incident," <https://docs.cloud.google.com/service-health/docs/incident-lifecycle>, n.d., accessed: 2025-12-01.
 - [35] OpenTelemetry Authors, "OpenTelemetry specification: Overview," <https://opentelemetry.io/docs/specs/otel/overview/>, 2025, overview of the OpenTelemetry project and core concepts. Accessed: 2025-11-28.
 - [36] H. Yan, Y. Chen, M. Ma, M. Wen, S. Lu, S. Zhang, T. Xu, R. Wang, C. Bansal, S. Rajmohan, C. Zhang, and D. Zhang, "An empirical study of production incidents in generative AI cloud services," *CoRR*, vol. abs/2504.08865, 2025, accepted to ISSRE 2025; preprint on arXiv. [Online]. Available: <https://arxiv.org/abs/2504.08865>
 - [37] M. Barletta, M. Cinque, C. Di Martino, Z. T. Kalbarczyk, and R. K. Iyer, "Mutiny! how does kubernetes fail, and what can we do about it?" in *2024 54th Annual IEEE/IFIP International Conference on Dependable Systems and Networks (DSN)*, 2024, pp. 1–14.
 - [38] Discord Engineering, "25% or 6 to 4: The 11/6/23 authentication outage," Nov. 2023, accessed: 2025-12-04. [Online]. Available: <https://discord.com/blog/authentication-outage>
 - [39] J. Graham-Cumming, "Details of the Cloudflare outage on July 2, 2019," Jul. 2019, accessed: 2025-12-04. [Online]. Available: <https://blog.cloudflare.com/details-of-the-cloudflare-outage-on-july-2-2019/>
 - [40] CrowdStrike, "External technical root cause analysis — channel file 291," Aug. 2024, accessed: 2025-12-04. [Online]. Available: <https://www.crowdstrike.com/wp-content/uploads/2024/08/Channel-File-291-Incident-Root-Cause-Analysis-08.06.2024.pdf>
 - [41] Spotify Engineering, "Incident report: Spotify outage on april 16, 2025," May 2025, accessed: 2025-12-04. [Online]. Available: <https://engineering.atspotify.com/2025/05/incident-report-spotify-outage-april-16>
 - [42] B. Dettelback, "About the Quay.io outage: Post mortem," Aug. 2020, accessed: 2025-12-04. [Online]. Available: <https://www.redhat.com/en/blog/about-the-quay.io-outage-post-mortem>
 - [43] S. Yao, J. Zhao, D. Yu, N. Du, I. Shafran, K. R. Narasimhan, and Y. Cao, "React: Synergizing reasoning and acting in language models," in *The Eleventh International Conference on Learning Representations*, 2023. [Online]. Available: https://openreview.net/forum?id=WE_vluYUL-X
 - [44] M. Chen, J. Tworek, H. Jun, Q. Yuan, H. P. de Oliveira Pinto, J. Kaplan, H. Edwards, Y. Burda, N. Joseph, G. Brockman, A. Ray, R. Puri, G. Krueger, M. Petrov, H. Khlaaf, G. Sastry, P. Mishkin, B. Chan, S. Gray, N. Ryder, M. Pavlov, A. Power, L. Kaiser, M. Bavarian, C. Winter, P. Tillet, F. P. Such, D. Cummings, M. Plappert, F. Chantzis, E. Barnes, A. Herbert-Voss, W. H. Guss, A. Nichol, A. Paino, N. Tezak, J. Tang, I. Babuschkin, S. Balaji, S. Jain, W. Saunders, C. Hesse, A. N. Carr, J. Leike, J. Achiam, V. Misra, E. Morikawa, A. Radford, M. Knight, M. Brundage, M. Murati, K. Mayer, P. Welinder, B. McGrew, D. Amodei, S. McCandlish, I. Sutskever, and W. Zaremba, "Evaluating large language models trained on code," *arXiv preprint arXiv:2107.03374*, 2021. [Online]. Available: <https://arxiv.org/abs/2107.03374>
 - [45] LangChain AI, "LangGraph: Build resilient, stateful multi-agent workflows for LLM applications," 2025, open-source framework for long-running, controllable LLM agents; integrates with LangChain. [Online]. Available: <https://github.com/langchain-ai/langgraph>
 - [46] TIOBE Software BV. TIOBE index for October 2025. Monthly

- updated indicator of the popularity of programming languages. [Online]. Available: <https://www.tiobe.com/tiobe-index/>
- [47] C. E. Jimenez, J. Yang, A. Wettig, S. Yao, K. Pei, O. Press, and K. R. Narasimhan, "SWE-bench: Can language models resolve real-world GitHub issues?" in *The Twelfth International Conference on Learning Representations*, 2024. [Online]. Available: <https://openreview.net/forum?id=VTF8yNQm66>
 - [48] C. Winston and R. Just, "A taxonomy of failures in tool-augmented LLMs," in *2025 IEEE/ACM International Conference on Automation of Software Test (AST)*, 2025, pp. 125–135. [Online]. Available: <https://doi.org/10.1109/AST66626.2025.00019>
 - [49] Q. Xiong, Y. Huang, Z. Jiang, Z. Chang, Y. Zheng, T. Li, and M. Li, "Butterfly effects in toolchains: A comprehensive analysis of failed parameter filling in LLM tool-agent systems," in *Findings of the Association for Computational Linguistics: EMNLP 2025*, C. Christodoulopoulos, T. Chakraborty, C. Rose, and V. Peng, Eds. Suzhou, China: Association for Computational Linguistics, Nov. 2025, pp. 16 712–16 729. [Online]. Available: <https://aclanthology.org/2025.findings-emnlp.907/>
 - [50] A. Gola, "Multi needle in a haystack," <https://blog.langchain.com/multi-needle-in-a-haystack/>, Mar. 2024, accessed: 2025-11-23.
 - [51] K. Hong, A. Troynikov, and J. Huber, "Context rot: How increasing input tokens impacts llm performance," Chroma, Tech. Rep., July 2025. [Online]. Available: <https://research.trychroma.com/context-rot>
 - [52] Y. Chen, H. Xie, M. Ma, Y. Kang, X. Gao, L. Shi, Y. Cao, X. Gao, H. Fan, M. Wen, J. Zeng, S. Ghosh, X. Zhang, C. Zhang, Q. Lin, S. Rajmohan, D. Zhang, and T. Xu, "Automatic root cause analysis via large language models for cloud incidents," in *Proceedings of the Nineteenth European Conference on Computer Systems*, ser. EuroSys '24. New York, NY, USA: Association for Computing Machinery, 2024, pp. 674–688. [Online]. Available: <https://doi.org/10.1145/3627703.3629553>
 - [53] M. Du, F. Li, G. Zheng, and V. Srikumar, "DeepLog: Anomaly detection and diagnosis from system logs through deep learning," in *Proceedings of the 2017 ACM SIGSAC Conference on Computer and Communications Security*, ser. CCS '17. New York, NY, USA: Association for Computing Machinery, 2017, pp. 1285–1298. [Online]. Available: <https://doi.org/10.1145/3133956.3134015>
 - [54] H. Ren, B. Xu, Y. Wang, C. Yi, C. Huang, X. Kou, T. Xing, M. Yang, J. Tong, and Q. Zhang, "Time-series anomaly detection service at Microsoft," in *Proceedings of the 25th ACM SIGKDD International Conference on Knowledge Discovery & Data Mining*, ser. KDD '19. New York, NY, USA: Association for Computing Machinery, 2019, pp. 3009–3017. [Online]. Available: <https://doi.org/10.1145/3292500.3330680>
 - [55] Z. Li, J. Chen, R. Jiao, N. Zhao, Z. Wang, S. Zhang, Y. Wu, L. Jiang, L. Yan, Z. Wang, Z. Chen, W. Zhang, X. Nie, K. Sui, and D. Pei, "Practical root cause localization for microservice systems via trace analysis," in *2021 IEEE/ACM 29th International Symposium on Quality of Service (IWQOS)*, 2021, pp. 1–10. [Online]. Available: <https://doi.org/10.1109/IWQOS52092.2021.9521340>
 - [56] S. Jha, S. Cui, S. S. Banerjee, T. Xu, J. Enos, M. Showerman, Z. T. Kalbarczyk, and R. K. Iyer, "Live forensics for HPC systems: A case study on distributed storage systems," in *Proceedings of the International Conference for High Performance Computing, Networking, Storage and Analysis*, ser. SC '20. IEEE Press, 2020. [Online]. Available: <https://doi.org/10.1109/SC41405.2020.00069>
 - [57] Y. Zhang, Z. Guan, H. Qian, L. Xu, H. Liu, Q. Wen, L. Sun, J. Jiang, L. Fan, and M. Ke, "CloudRCA: A root cause analysis framework for cloud computing platforms," in *Proceedings of the 30th ACM International Conference on Information & Knowledge Management*, ser. CIKM '21. New York, NY, USA: Association for Computing Machinery, 2021, pp. 4373–4382. [Online]. Available: <https://doi.org/10.1145/3459637.3481903>
 - [58] Y. Jiang, C. Zhang, S. He, Z. Yang, M. Ma, S. Qin, Y. Kang, Y. Dang, S. Rajmohan, Q. Lin, and D. Zhang, "Xpert: Empowering incident management with query recommendations via large language models," in *Proceedings of the IEEE/ACM 46th International Conference on Software Engineering*, ser. ICSE '24. New York, NY, USA: Association for Computing Machinery, 2024. [Online]. Available: <https://doi.org/10.1145/3597503.3639081>
 - [59] D. Goel, F. Husain, A. Singh, S. Ghosh, A. Parayil, C. Bansal, X. Zhang, and S. Rajmohan, "X-lifecycle learning for cloud incident management using llms," in *Companion Proceedings of the 32nd ACM International Conference on the Foundations of Software Engineering*, ser. FSE 2024. New York, NY, USA: Association for Computing Machinery, 2024, pp. 417–428. [Online]. Available: <https://doi.org/10.1145/3663529.3663861>
 - [60] P. Jin, S. Zhang, M. Ma, H. Li, Y. Kang, L. Li, Y. Liu, B. Qiao, C. Zhang, P. Zhao, S. He, F. Sarro, Y. Dang, S. Rajmohan, Q. Lin, and D. Zhang, "Assess and summarize: Improve outage understanding with large language models," in *Proceedings of the 31st ACM Joint European Software Engineering Conference and Symposium on the Foundations of Software Engineering*, ser. ESEC/FSE 2023. New York, NY, USA: Association for Computing Machinery, 2023, pp. 1657–1668. [Online]. Available: <https://doi.org/10.1145/3611643.3613891>
 - [61] X. Zhang, T. Mittal, C. Bansal, R. Wang, M. Ma, Z. Ren, H. Huang, and S. Rajmohan, "FLASH: A workflow automation agent for diagnosing recurring incidents," Microsoft Research Technical Report (preprint), 2024. [Online]. Available: https://www.microsoft.com/en-us/research/wp-content/uploads/2024/10/FLASH_Paper.pdf
 - [62] Y. Han, Q. Du, Y. Huang, J. Wu, F. Tian, and C. He, "The potential of one-shot failure root cause analysis: Collaboration of the large language model and small classifier," in *Proceedings of the 39th IEEE/ACM International Conference on Automated Software Engineering*, ser. ASE '24. New York, NY, USA: Association for Computing Machinery, 2024, pp. 931–943. [Online]. Available: <https://doi.org/10.1145/3691620.3695475>
 - [63] C. Pei, Z. Wang, F. Liu, Z. Li, Y. Liu, X. He, R. Kang, T. Zhang, J. Chen, J. Li, G. Xie, and D. Pei, "Flow-of-action: SOP enhanced LLM-based multi-agent system for root cause analysis," in *Companion Proceedings of the ACM on Web Conference 2025*, ser. WWW '25. New York, NY, USA: Association for Computing Machinery, 2025, pp. 422–431. [Online]. Available: <https://doi.org/10.1145/3701716.3715225>
 - [64] Y. Bei, W. Zhang, S. Wang, W. Chen, S. Zhou, H. Chen, Y. Li, J. Bu, S. Pan, Y. Yu, I. King, F. Karray, and P. S. Yu, "Graphs meet AI agents: Taxonomy, progress, and future opportunities," 2025. [Online]. Available: <https://arxiv.org/abs/2506.18019>
 - [65] B. Jin, C. Xie, J. Zhang, K. K. Roy, Y. Zhang, Z. Li, R. Li, X. Tang, S. Wang, Y. Meng, and J. Han, "Graph chain-of-thought: Augmenting large language models by reasoning on graphs," in *Findings of ACL*, 2024, pp. 163–184. [Online]. Available: <https://aclanthology.org/2024.findings-acl.11.pdf>
 - [66] J. Sun, C. Xu, L. Tang, S. Wang, C. Lin, Y. Gong, L. Ni, H.-Y. Shum, and J. Guo, "Think-on-graph: Deep and responsible reasoning of large language model on knowledge graph," in *The Twelfth International Conference on Learning Representations*, 2024. [Online]. Available: <https://openreview.net/forum?id=nnVO1PvbTv>
 - [67] L. Chen, P. Tong, Z. Jin, Y. Sun, J. Ye, and H. Xiong, "Plan-on-graph: Self-correcting adaptive planning of large language model on knowledge graphs," in *Proceedings of the 38th International Conference on Neural Information Processing Systems*, ser. NIPS '24. Red Hook, NY, USA: Curran Associates Inc., 2025. [Online]. Available: <https://doi.org/10.52202/079017-1189>
 - [68] X. Tan, X. Wang, Q. Liu, X. Xu, X. Yuan, and W. Zhang, "Paths-over-graph: Knowledge graph empowered large language model reasoning," in *Proceedings of the ACM on Web Conference 2025*, ser. WWW '25. New York, NY, USA: Association for Computing Machinery, 2025, pp. 3505–3522. [Online]. Available: <https://doi.org/10.1145/3696410.3714892>
 - [69] Z. Chen, R. Tang, G. Deng, F. Wu, J. Wu, Z. Jiang, V. Prasanna, A. Cohan, and X. Wang, "LocAgent: Graph-guided LLM agents for code localization," in *Proceedings of the 63rd Annual Meeting of the Association for Computational Linguistics (Volume 1: Long Papers)*, W. Che, J. Nabende, E. Shutova, and M. T. Pilehvar, Eds. Vienna, Austria: Association for Computational Linguistics, Jul. 2025, pp. 8697–8727. [Online]. Available: <https://aclanthology.org/2025.acl-long.426/>
 - [70] J. Pu, Y. Li, Z. Chen, J. Liu, Z. Jiang, J. Chen, R. Shi, Z. Zheng, and T. Zhang, "ErrorPrism: Reconstructing error propagation paths in cloud service systems," *arXiv preprint arXiv:2509.26463*, 2025. [Online]. Available: <https://arxiv.org/abs/2509.26463>
 - [71] L. Pham, H. Ha, and H. Zhang, "Root cause analysis for microservice system based on causal inference: How far are we?" in *Proceedings of the 39th IEEE/ACM International Conference on Automated Software Engineering*, ser. ASE '24. New York, NY, USA: Association for Computing Machinery, 2024, pp. 706–715. [Online]. Available: <https://doi.org/10.1145/3691620.3695065>